Veterinary Microbiology 305 (2025) 110535

Contents lists available at ScienceDirect

Veterinary Microbiology

journal homepage: www.elsevier.com/locate/vetmic

Curcumin activates the JAK-STAT signaling pathway to enhance the innate immune response against porcine epidemic diarrhea virus infection in vivo and in vitro

Qiancheng Jiang [a,1], Xiangyang Liu [a,b,1], Jianbo Yuan [a,1], Shujuan Zhang [a], Yiling Zhang [a,c], Zifei Kan [a,d], Zheng Niu [a,e], Li Zhang [a], Xia Hu [a], Yang Zhou [a,b], Jing Wang [a], Fei Li [a], Lijing Cao [f], Xingcui Zhang [a,g,*], Chenghong Lei [b,*], Zhenhui Song [a,g,*]

[a] College of Veterinary Medicine, Southwest University, Chongqing, China
[b] College of Veterinary Medicine, Xinjiang Agricultural University, Urumqi, China
[c] College of Animal Science and Technology, Chongqing Three Gorges Vocational College, Chongqing, China
[d] School of Medicine, University of Electronic Science and Technology of China, Chengdu, China
[e] College of Veterinary Medicine, Northwest A and F University, Shanxi, China
[f] Rongchang Vocational Education Center, Chongqing, China
[g] Immunology Research Center, Medical Research Institute, Southwest University, Chongqing, China

ARTICLE INFO

Keywords:
Curcumin
PEDV
JAK-STAT signaling pathway
Innate immunity
Antiviral activity

ABSTRACT

Porcine epidemic diarrhea (PED) is a highly pathogenic infectious disease caused by porcine epidemic diarrhea virus (PEDV), which has caused significant economic losses to the global pig industry. Due to the high mutability of the PEDV genome, the development of effective vaccines or drugs to prevent and control PEDV is still facing great difficulties. In this study, we found that the natural compound curcumin showed effective antiviral activity against PEDV in VERO-E6 and IPEC-J2 cells. The Janus Kinase-Signal Transducer and Activator of Transcription (JAK-STAT) signaling pathway was screened by transcriptomics as a potential innate immune mechanism of IPEC-J2 cells against PEDV infection. For PEDV, a highly pathogenic virus, cellular autoimmune response is not sufficient to fight against its infection. Our results demonstrated that curcumin could exert antiviral effects by enhancing the JAK-STAT cascade reaction mediated by type I interferon IFN-α and IFN-β in IPEC-J2 cells. In vivo experiments further confirmed the protective effect of curcumin on PEDV-infected piglets and its positive regulation of the JAK-STAT signaling pathway. In vivo, curcumin prophylaxis significantly enhanced IFN-α and IFN-β-induced JAK-STAT signaling and the production of interferon-stimulated genes (ISGs), and increased the innate immune response, thus exerting antiviral effects effectively. In conclusion, our data indicate that curcumin can effectively resist PEDV infection in IPEC-J2 cells and piglets, which provides a new reference for the development of anti-PEDV drugs with important application prospects.

1. Introduction

PED is an acute and highly contagious porcine enteroviral disease that spreads among pigs of all ages and causes symptoms such as vomiting, watery diarrhea, anorexia, and weight loss, affecting nursing piglets in particular, and seriously hampering the development of the pig industry (Li et al., 2012). The pathogen PEDV is a porcine enteropathogenic coronavirus, which was first reported in England in the 1970s (Wood, 1977), and subsequently became widespread worldwide. PEDV has been detected in China since the 1980s, and started to become

* Correspondence to: College of Veterinary Medicine, Southwest University, , No. 160 Xueyuan Road, Rongchang District, Chongqing 402460, China.
** Corresponding author.
E-mail addresses: 3115264032@qq.com (Q. Jiang), 798304505@qq.com (X. Liu), 2038222182@qq.com (J. Yuan), 3466396106@qq.com (S. Zhang), 1491141262@qq.com (Y. Zhang), 970949352@qq.com (Z. Kan), 1029610286@qq.com (Z. Niu), 3045706471@qq.com (L. Zhang), 2550418434@qq.com (X. Hu), 1320517712@qq.com (Y. Zhou), 2860235766@qq.com (J. Wang), 1821106023@qq.com (F. Li), 517296566@qq.com (L. Cao), zhangxc923@swu.edu.cn (X. Zhang), leichxjnd@aliyun.com (C. Lei), szh7678@126.com (Z. Song).
[1] These authors contributed equally to the work.

https://doi.org/10.1016/j.vetmic.2025.110535
Received 28 February 2025; Received in revised form 22 April 2025; Accepted 24 April 2025
Available online 25 April 2025

Table 1
Primers used for RT-qPCR.

Primers	Sequences 5'-3'
PEDV N-F	CGATGATCTGGTGGCTGCTGTC
PEDV N-R	TTCCTGCTTAGGCTTCTGCTGTTG
STAT1-F	CCTTGCAGAATAGAGAACATGATAC
STAT1-R	CCTTTCTCTTGTTGTCAAGCATT
MX1-F	ATCTGTAAGCAGGAGACCATCAACTTG
MX1-R	CTCGCCACGTCCACTATCTTGTC
ISG15-F	GGCAGCACAGTCCTGTTGATGG
ISG15-R	TGCGTCAGCCAGACCTCATAGG
OASL-F	CTGGTGGCATTTCTGTGCT
OASL-R	AGATGGTGAAGGCGATGG
β actin-F	CTCTTCCAGCCCTCCTTCC
β actin-R	GGTCCTTGCGGATGTCG

a large-scale epidemic in China in 2010. Due to its high degree of variability and complexity, the vaccines and drugs developed in the past were only effective against the classical PEDV strains that were prevalent before 2010, but not against the currently prevalent mutated strains, even some of the vaccinated herds are still infected with PEDV, which greatly reduces the immunization effect of conventional vaccines (Wang et al., 2020). Therefore, it is crucial to find effective anti-PEDV drugs to prevent PEDV infection.

Type I IFN-mediated innate immune response is an important means for host cells to resist viral invasion. Upon detection of a virus by a pathogen recognition receptor, IFN is released and binds to specific receptors on the cell surface, and the JAK-STAT pathway is activated, leading to the production of a series of downstream antiviral ISGs (Mahjoor et al., 2023). The JAK-STAT signaling pathway is responsible for transmitting chemical signals from the outside of the cell to the nucleus, thus promoting the transcription of specific genes downstream of the pathway, and consists of the cellular receptor (IFNAR1 and IFNAR2), the JAK protein (JAK1, JAK2, JAK3, and TYK2), and the STAT protein(STAT1, STAT2, STAT3, STAT4, STAT5A, STAT5B, and STAT6) (Aaronson and Horvath, 2002). IFNAR1 and IFNAR2 are associated with JAK1, and upon their activation, they recruit STAT proteins (Decker et al., 2005). The heterodimer formed by STAT1 and STAT2 binds to interferon regulatory factor 9 (IRF9) in the cytoplasm, forming the interferon-stimulated gene factor 3 (ISGF3) complex. This complex then translocates to the nucleus, where it binds to the interferon-stimulated response element (ISRE) DNA sequence, triggering the transcription of ISGs. This cascade of events initiates a series of antiviral responses (Schneider et al., 2014). STAT1 is not only a critical factor in activating the JAK-STAT signaling pathway but also a key regulator of interferon-stimulated genes (ISGs) such as ISG15, MX1, and OASL, which exhibit potent antiviral activity against PEDV (Schneider et al., 2014; Xu et al., 2023). As recently reported, the transcription of STAT1 and STAT4 was significantly upregulated in IPEC-J2 cells 24 h post-PEDV infection. Western blot analysis further demonstrated that STAT1 levels gradually increased with prolonged PEDV infection. Overexpression of STAT1 significantly inhibited PEDV infection, whereas chemical inhibition or knockdown of STAT1 promoted PEDV replication by downregulating the expression of ISGs (Xu et al., 2023). As a highly pathogenic coronavirus, PEDV has evolved strategies to counteract the host's IFN-mediated innate antiviral immunity. The PEDV nonstructural protein nsp7 can sequester the interaction between karyopherin α1 (KPNA1) and STAT1, thereby blocking the nuclear translocation of ISGF3 and suppressing type I IFN-mediated JAK-STAT signaling (Zhang et al., 2022). Although PEDV infection upregulates the transcriptional levels of IFITM1, MX1, OASL, and ISG15, it significantly reduces the expression of OASL and ISG15 induced by the IFN agonist poly(I·C). Furthermore, PEDV infection markedly decreases poly (I·C)-induced STAT1 phosphorylation and nuclear localization, thereby inhibiting IFN-mediated antiviral responses (Xu et al., 2023).

Natural compounds have garnered heightened interest among researchers due to several factors, including their abundant sources, reduced adverse effects, and comparatively lower costs (Liang et al., 2024). Curcumin, a hydrophobic, low-molecular-weight polyphenolic compound, is present in turmeric rhizomes, which are commonly found in Asian countries. It is the primary component of turmeric powder, a substance that is widely utilized both as a culinary spice and a component of traditional medicine. Numerous studies have demonstrated that curcumin exhibits potent antiviral activity and modulates the innate immune response. Specifically, it has been demonstrated to inhibit classical swine fever virus (CSFV) replication in a dose-dependent manner and to promote innate immune responses independently of the NF-κB signaling pathway (Gao et al., 2021). Additionally, a film-forming spray containing curcumin has been shown to exert multiple inhibitory effects against Severe Acute Respiratory Syndrome Coronavirus 2 (SARS-CoV-2) infection by enhancing mucosal innate immunity and suppressing the binding of SARS-CoV-2 to angiotensin-converting enzyme-2 (ACE-2) on target cells (Nittayananta et al., 2024). Curcumin exhibits antiviral activity against SARS-CoV-2 (Marín-Palma et al., 2021), Transmissible Gastroenteritis Virus (TGEV) (Li et al., 2020), and Porcine Delta Coronavirus (PDCoV) (Wang et al., 2023). However, its efficacy against PEDV, another member of the *Coronaviridae* family, remains to be investigated.

In this study, we reported that curcumin exhibited good anti-PEDV activity both in vivo and in vitro, and demonstrated that curcumin exerts its potent antiviral effects through immune enhancement by enhancing the host cell type I IFN: IFN-α and IFN-β-mediated JAK/STAT cascade reaction to promote the production of antiviral ISGs. These findings are expected to provide insights into the clinical application of curcumin as an anti-PEDV infection drug.

2. Materials and methods

2.1. Cells, viruses, antibodies, and reagents

African green monkey kidney cells (VERO-E6) and porcine intestinal epithelial cells (IPEC-J2) were purchased from Suer Biotechnology Co., Ltd. (Shanghai, China). Both cell lines were cultured in DMEM medium (Gibco, USA) supplemented with 10 % fetal bovine serum (BI, Israel) and maintained at 37°C in a 5 % CO_2 incubator. The PEDV-LJX strain and mouse anti-PEDV N monoclonal antibody were kindly provided by Dr. Liu Guangliang from the Lanzhou Veterinary Research Institute, Chinese Academy of Agricultural Sciences. Rabbit anti-STAT1 polyclonal antibody and mouse anti-P-STAT1 polyclonal antibody were purchased from Bioss (Beijing, China). Horseradish peroxidase (HRP)-conjugated goat anti-mouse secondary antibody, HRP-conjugated goat anti-rabbit secondary antibody, mouse anti-β-actin monoclonal antibody, and Cy3-conjugated goat anti-mouse fluorescent secondary antibody were obtained from Proteintech (Wuhan, China). DAPI and Alexa Fluor 647-conjugated goat anti-rabbit fluorescent secondary antibody were purchased from Beyotime (Shanghai, China). Curcumin was acquired from Sangon Biotech Co., Ltd. (Shanghai, China). Porcine IFN-α ELISA kit (MM-037802) and porcine IFN-β ELISA kit (MM-036802) were purchased from Jiangsu Meimian Industrial Co., Ltd.

2.2. Cell viability assay

VERO-E6 and IPEC-J2 cells were seeded into 96-well plates at a density of 2×10^4 cells per well and treated with varying concentrations of curcumin (4, 8, 16, 32, 64, and 128 μM). After 24 h of treatment, CCK-8 reagent (Addison Biotechnology Co., Ltd., Jiangsu, China) was added to each well and incubated for 1 hour. The absorbance at 450 nm was measured using a microplate reader (Bio-Rad, USA). Cell viability was calculated using the following formula: Cell viability (%) = [OD (drug-treated) − OD (blank)] / [OD (control) − OD (blank)] × 100.

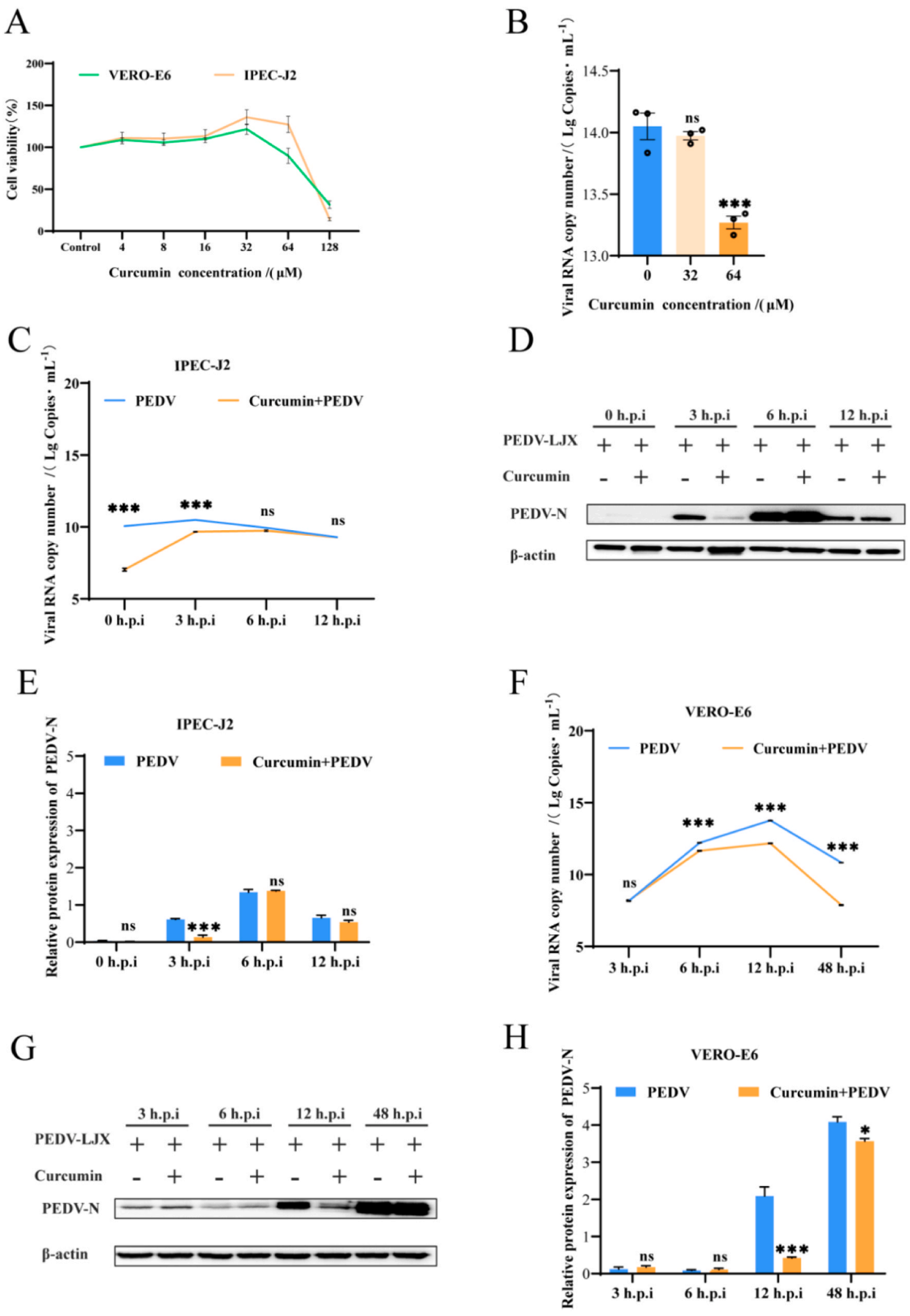

Fig. 1. Cytotoxicity and anti-PEDV activity of curcumin in VERO-E6 and IPEC-J2 cells. (A) Vero and IPEC-J2 cells were treated with varying concentrations of curcumin (4, 8, 16, 32, 64, and 128 μM) for 24 h, and cell viability was assessed using the CCK-8 assay. (B) Vero cells pretreated with 32 μM or 64 μM curcumin for 3 h were infected with PEDV for 24 h, and the copy number of the PEDV N gene was measured. (C) Changes in the copy number of the PEDV N gene at different time points post-infection in IPEC-J2 cells pretreated with 64 μM curcumin for 3 h. (D, E) Changes in PEDV N protein expression at different time points post-infection in IPEC-J2 cells pretreated with 64 μM curcumin for 3 h. (F) Changes in the copy number of the PEDV N gene at different time points post-infection in Vero cells pretreated with 64 μM curcumin for 3 h. (G, H) Changes in PEDV N protein expression at different time points post-infection in Vero cells pretreated with 64 μM curcumin for 3 h. Asterisks in the figure indicate significant differences (*: $P < 0.05$; **: $P < 0.01$; ***: $P < 0.001$; ns: not significant).

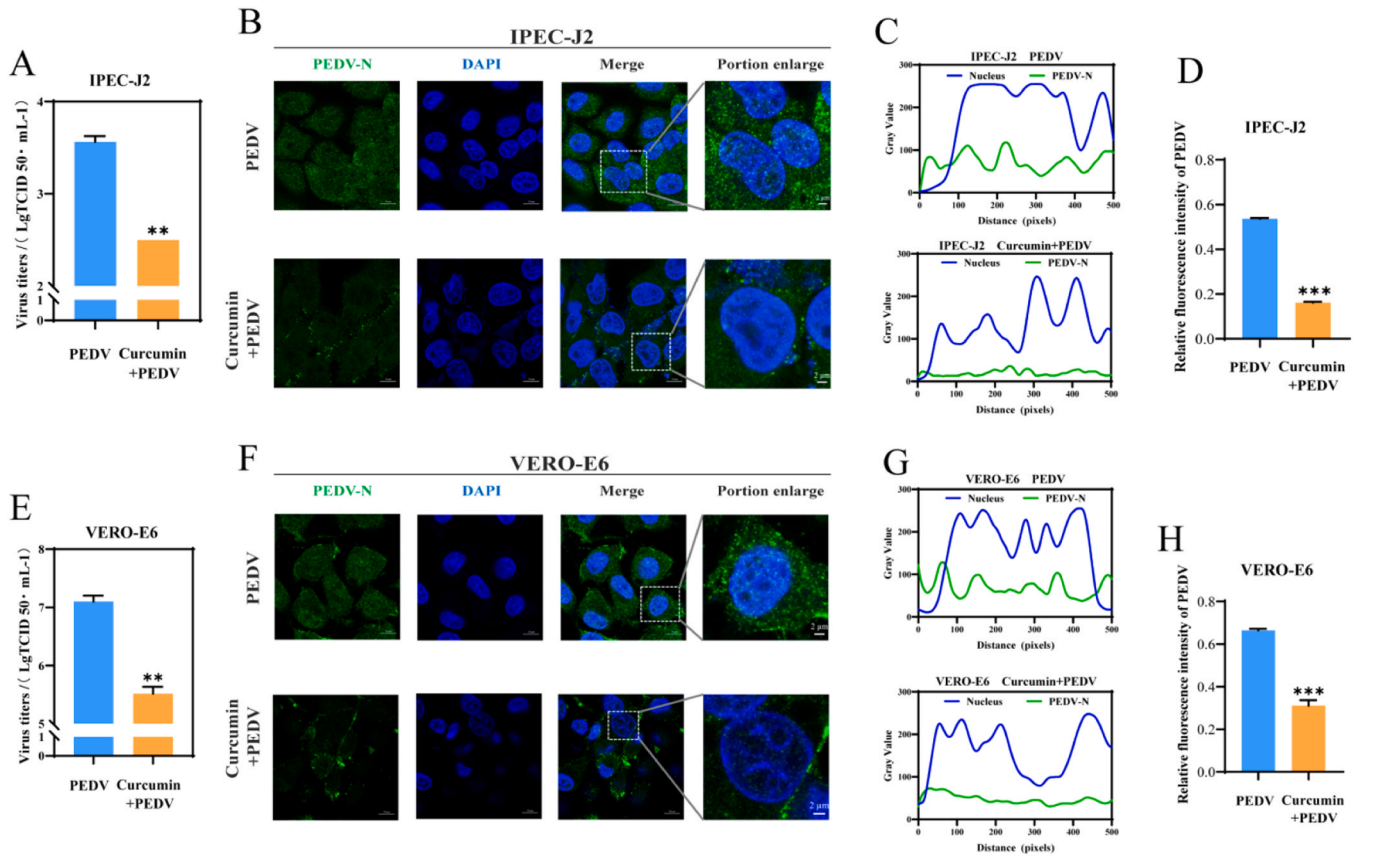

Fig. 2. Effect of Curcumin on the titer and distribution of PEDV virus.

2.3. RNA extraction and quantitative real-time PCR

Total RNA was extracted from each cell sample and reverse-transcribed into cDNA using PrimeScript™ RT Master Mix (TaKaRa, Beijing, China). Specific primers targeting the PEDV N gene (GenBank Number: MK252703.1) were designed (Table 1), and the copy number of the PEDV N gene was quantified using absolute quantitative real-time PCR. The linear relationship between the cycle threshold (CT) values and the copy number was analyzed using the random matrix method in Bio-Rad CFX Manager software, and the PEDV N gene copy number was calculated. The full sequences of STAT1, ISG15, MX1, OASL, and β-actin genes were downloaded from NCBI. Using β-actin as the internal reference, cDNA was subjected to qPCR amplification. The reaction mixture consisted of 5.0 μL SYBR PreMix ExTaq II, 0.4 μL forward primer, 0.4 μL reverse primer, 1 μL cDNA, and 3.2 μL H_2O. The reaction protocol was as follows: 95°C for 30 s, followed by 40 cycles of 95°C for 5 s and 55°C for 30 s. Each sample was analyzed in at least three replicates. The primers used are listed in Table 1, and the relative mRNA expression levels were analyzed using the $2^{-\Delta\Delta Ct}$ method.

2.4. Western blot analysis

The protein samples were then quantified using a BCA Protein Concentration Assay Kit (Beyotime, Shanghai, China). The quantitatively denatured proteins were separated by electrophoresis using SDS-PAGE gels (Beyotime, Shanghai, China) and subsequently transferred onto polyvinylidene difluoride (PVDF) membranes (Merck Millipore, USA). The PVDF membranes were then blocked with 5 % skimmed milk powder for 1.5 h and incubated with the corresponding primary antibodies at 4°C overnight. The next step involved incubating the membranes with the corresponding secondary antibodies for 1 h at room temperature. Finally, the Western blotting results were visualized by FX5 imaging system (VILBER, Israel) using BeyoECL Star (Beyotime, Shanghai, China).

2.5. Virus titration

Vero cells were cultivated in a 96-well plate and subjected to infection with PEDV through a tenfold serial dilution. Following a 1-h incubation at 37°C, the medium was replaced with fresh DMEM basal medium. The cells were then maintained for an additional 96 h. Cytopathic effects (CPE) were examined under a microscope, and the viral titer was calculated employing the Reed-Muench method.

2.6. Indirect immunofluorescence assay

VERO-E6 and IPEC-J2 cells were seeded onto coverslip-containing 24-well plates at a density of 2×10^4 cells per well. Following experimental group treatments, cells were harvested and fixed with 4 % paraformaldehyde (200 μL/well) at room temperature for 25 min. Permeabilization was performed using 0.3 % Triton X-100 (200 μL/well) at 4°C for 10 min, followed by blocking with 5 % BSA diluted in PBST (200 μL/well) at room temperature for 1 h. Subsequently, cells were incubated with PEDV N Mouse Anti-Monoclonal Antibody at 4°C overnight. After washing, Alexa Fluor 647-conjugated goat anti-mouse secondary antibody (1:500 dilution) was applied and incubated at 37°C for 1 h under light-protected conditions. Nuclear counterstaining was performed with DAPI (200 μL/well) at ambient temperature for 10 min in darkness. Fluorescent images were acquired using a laser scanning confocal microscope (ZEISS, Germany). Each experiment contained at least three independent replicates per sample.

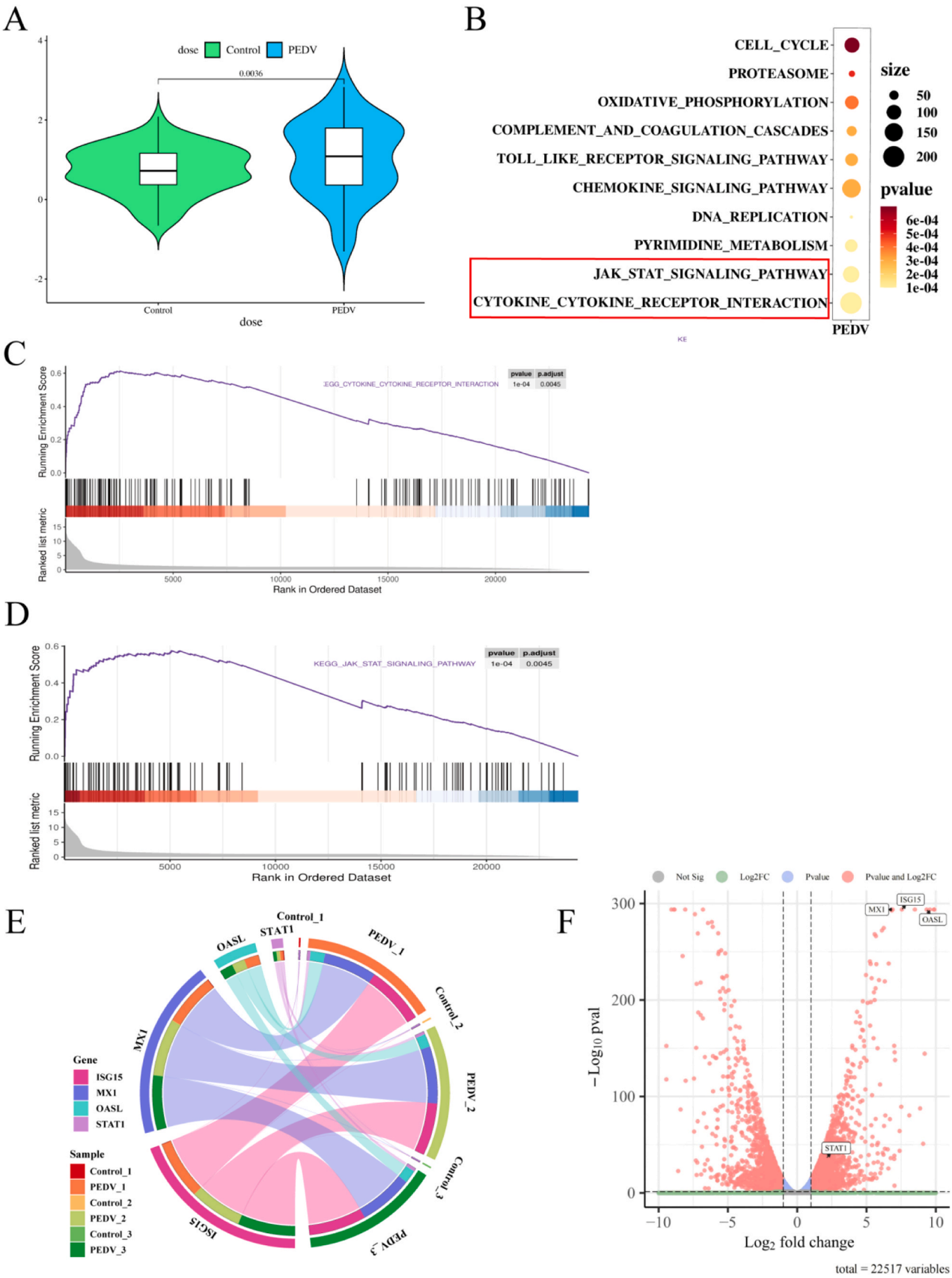

Fig. 3. Transcriptomic Analysis of the Correlation Between PEDV Infection and the JAK-STAT Signaling Pathway. Violin plot analysis of DEGs. (B-D) GSEA demonstrating the association of PEDV infection with the Cytokine-cytokine receptor interaction and JAK-STAT signaling pathway. (E) Circos plot illustrating the correlation between PEDV infection and key genes (STAT1, MX1, ISG15, and OASL) involved in the JAK-STAT signaling pathway. (F) Volcano plot showing the differential expression of PEDV infection-related genes (MX1, ISG15, OASL, and STAT1).

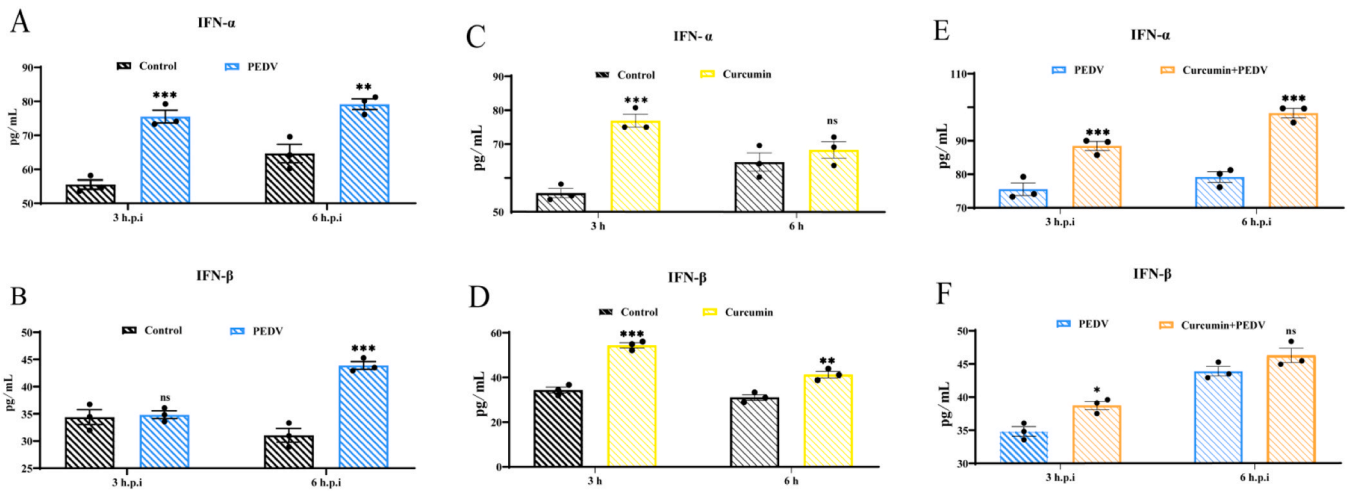

Fig. 4. Effects of PEDV infection, Curcumin-treated physiological conditions and Curcumin pretreated PEDV-infected conditions on IFN-α and IFN-β secretion levels in IPEC-J2 cells. (A-B) IFN-α, IFN-β secretion in IPEC-J2 cells at 3 h.p.i. and 6 h.p.i. of PEDV infection. (C-D) Changes in IFN-α, IFN-β secretion levels in cells after Curcumin treatment for 3 h under physiological conditions. (E-F) Changes in the secretion levels of IFN-α and IFN-β under the condition of PEDV infection by Curcumin pretreatment. Asterisks in the figure indicate significant differences (*: $P < 0.05$; **: $P < 0.01$; ***: $P < 0.001$; ns: not significant).

2.7. Transcriptomics analysis

Total RNA was isolated and purified from the jejunum of normal and PEDV-infected piglets, which were collected and preserved by our research group, using TRIzol reagent (TaKaRa, Beijing, China) according to the manufacturer's instructions. The concentration and purity of RNA in each sample were quantified using a NanoDrop ND-1000 spectrophotometer (NanoDrop, Wilmington, DE, USA). RNA integrity was assessed using the Agilent 2100 Bioanalyzer, with samples having an RNA Integrity Number (RIN) > 7.0 considered suitable for further analysis. Poly(A) RNA was purified from 5 μg of total RNA using Poly-T oligo-attached magnetic beads. The purified Poly(A) RNA was then fragmented into small pieces using divalent cations under elevated temperature. The fragmented RNA was reverse-transcribed into cDNA, and second-strand cDNA synthesis was performed using Escherichia coli DNA polymerase I, RNase H, and dUTP to generate uracil-labeled complementary DNA. An adenine (A) tail was added to the 3' end of each strand, followed by ligation to modified Illumina multiplex barcode adapters to minimize sequence-dependent bias and amplification noise. Size selection was performed using AMPure XP beads. The uracil-labeled cDNA was treated with UDG enzyme for thermal degradation, and the adapter-ligated fragments were amplified by PCR under the following conditions: initial denaturation at 95°C for 3 min; 8 cycles of denaturation at 98°C for 15 s, annealing at 60°C for 15 s, and extension at 72°C for 30 s; and a final extension at 72°C for 5 min. The final cDNA libraries had an average insert size of approximately 300 bp (± 50 bp). Paired-end sequencing was performed on the Illumina HiSeq 4000 platform (LC Bio, China) following the manufacturer's recommended protocol. Each sample was analyzed in at least three replicates.

2.8. Enzyme-linked immunosorbent assay (ELISA)

The cell culture fluid was collected into a sterile EP tube and subjected to centrifugation at 4°C at 2000 rpm for 20 min. to collect the upper layer. An ELISA kit was used to detect IFN-α and IFN-β, respectively. All experimental operations were performed according to the manufacturer's instructions. Each sample was repeated at least three times.

2.9. Animal experiment

Twenty PEDV-negative piglets were obtained from a small pig farm in Rongchang (Chongqing, China) and randomly divided into four groups: negative control group (NC), PEDV-positive control group (PEDV), curcumin group (curcumin), and curcumin-protected group (curcumin-PEDV), each group n = 5. The piglets were acclimatized and fed for 48 h prior to treatment, and the groups were placed in different isolation rooms to prevent cross-infection. In the morning, the negative and PEDV groups were given oral PBS, the curcumin and curcumin-protected groups were given 0.5 mg/kg curcumin, and after 3 h, the curcumin-PEDV groups were given 10 mL/kg PEDV-LJX solution with a viral titer of 1×10^5 $TCID_{50}$/mL, and the negative control and curcumin groups were given oral PBS. All piglets were euthanized on day 4 of treatment, and intestinal lesions were recorded by necropsy, and tissue samples from different intestinal segments were collected for subsequent experiments. All animal experiments were approved by Southwest University's Institutional Animal Care and Use Committee (Animal Protocol Approval Number: IACUC-20230509–02) and followed the National Institutes of Health's Animal Performance Guidelines.

2.10. Statistical analysis

Data were analyzed using GraphPad Prism 8.0 (GraphPad Software, San Diego, CA, USA). All experiments were performed three or more times and experimental data are presented as mean ± standard deviation (SD). Ns indicates $P > 0.05$, insignificant difference; *, # indicates $P < 0.05$, significant difference; **, ## indicates $P < 0.01$, highly significant difference; ***, ### indicates $P < 0.001$, highly significant difference.

3. Results

3.1. Curcumin inhibits PEDV infection in Vero and IPEC-J2 in vitro

Before conducting antiviral experiments, the cytotoxicity of curcumin was assessed using the CCK-8 assay. The results showed that when the concentration of curcumin ranged between 32 μM and 64 μM, the relative cell viability of IPEC-J2 consistently exceeded 100 %, while that of VERO-E6 remained above 80 % (Fig. 1A). To determine the optimal working concentration of curcumin for inhibiting PEDV infection, Vero cells were pretreated with 32 μM or 64 μM curcumin for 3 h, followed by PEDV infection for 24 h (MOI: 0.1). RT-qPCR results revealed that treatment with 64 μM curcumin significantly reduced the copy number of the PEDV N gene, whereas 32 μM curcumin had no significant effect

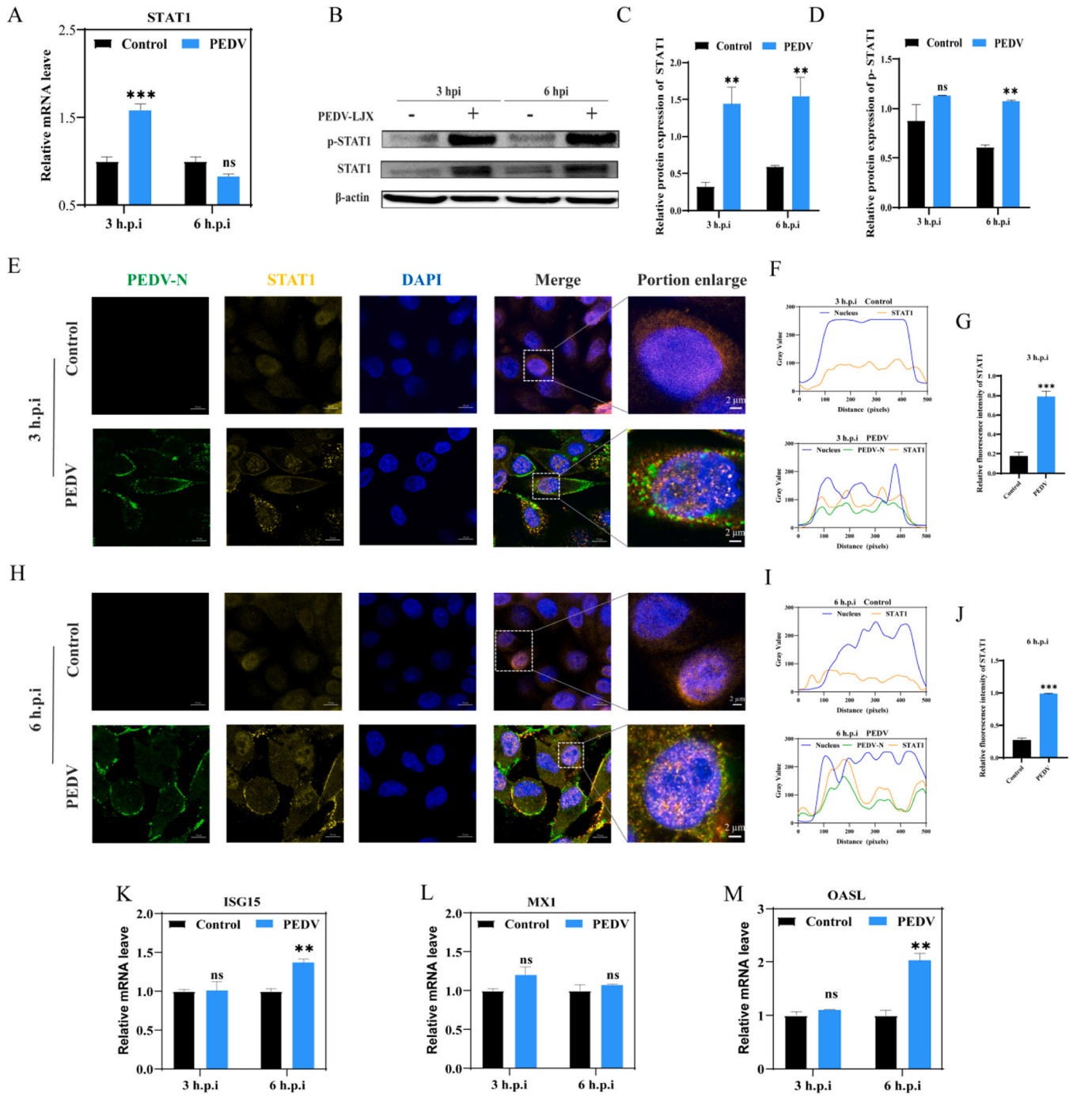

Fig. 5. Effects of PEDV Infection on STAT1 and ISGs (ISG15, MX1, OASL) in IPEC-J2 Cells. (A) Changes in the transcription levels of STAT1 at 3 h.p.i. and 6 h.p.i. following PEDV infection. (B-D) Alterations in total STAT1 protein levels, phosphorylated STAT1 protein levels at 3 h.p.i. and 6 h.p.i. after PEDV infection. (E-J) Nuclear localization of STAT1 at 3 h.p.i. and 6 h.p.i. following PEDV infection. (K-M) Changes in the transcription levels of ISG15, MX1, and OASL at 3 h.p.i. and 6 h.p.i. after PEDV infection. Asterisks indicate significant differences (*: $P < 0.05$; **: $P < 0.01$; ***: $P < 0.001$; ns: not significant).

on PEDV (Fig. 1B). Therefore, 64 μM curcumin was selected as the optimal working concentration for subsequent experiments. RT-qPCR and Western blot analyses demonstrated that the most significant inhibitory effect of curcumin on PEDV in IPEC-J2 cells occurred at 3 hour post-infection (h.p.i.) (Fig. 1C-E), while in Vero cells, the most pronounced inhibition was observed at 12 h.p.i. (Fig. 1F-H). TCID50 and immunofluorescence assay (IFA) further confirmed the antiviral activity of curcumin, showing that curcumin significantly reduced the expression levels of PEDV-N protein in both IPEC-J2 and Vero cells and decreased the nuclear localization of PEDV (Fig. 2). These results indicate that 64 μM curcumin effectively inhibits PEDV infection in Vero and IPEC-J2 cells, reduces viral titers, and diminishes viral localization in the nucleus.

Culture supernatants were collected for viral titer and the results are expressed as TCID50.IFA images show the viral N protein in green and the nuclei in blue. (A) PEDV virus titer in the supernatant of. IPEC-J2 cells 3 h.p.i. (B-D) PEDV-N distribution in 3 h.p.i. IPEC-J2 cells. (E) PEDV virus titers in supernatants of Vero cells 12 h.p.i. (F-H) PEDV-N distribution in Vero cells at 12 h.p.i. Asterisks in the figure indicate significant differences (*: $P < 0.05$; **: $P < 0.01$; ***: $P < 0.001$; ns: not

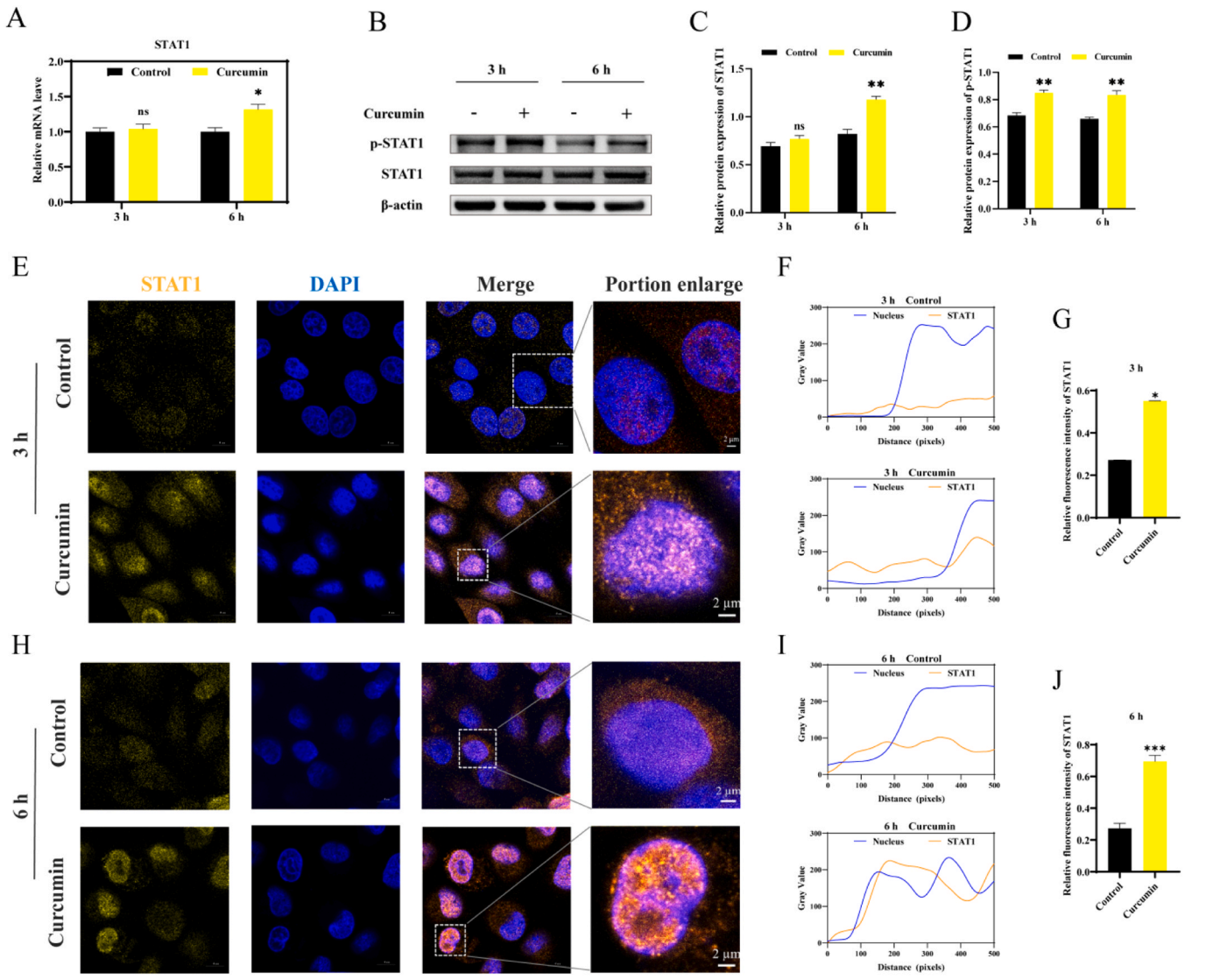

Fig. 6. Changes in STAT1 under physiological conditions after curcumin treatment. (A) Changes in the transcriptional level of STAT1 at 3 h and 6 h post-curcumin treatment. (B-D) Changes in total STAT1 protein levels and phosphorylation status at 3 h and 6 h post-curcumin treatment. (E-J) Changes in the nuclear localization of STAT1 at 3 h and 6 h post-curcumin treatment. Asterisks in the figure indicate significant differences (*: $P < 0.05$; **: $P < 0.01$; ***: $P < 0.001$; ns: not significant).

significant).

3.2. *Transcriptomics predicts correlation between PEDV infection and the JAK-STAT pathway*

The transcriptome data were normalized using z-score transformation and subjected to principal component analysis (PCA). The results showed that the samples accounted for 82.02 % of the variance in principal component 1 (PCA1) and 17.53 % in principal component 2 (PCA2), with a cumulative contribution of 99.55 %. This indicates excellent sample reproducibility, with no outliers, suggesting that the experimental results are highly reproducible and reliable (Fig. S1). Violin plots were generated to analyze the distribution of differentially expressed genes (DEGs). Compared to the blank control group, the gene distribution in PEDV-infected samples was broader, primarily distributed around the median, while the blank control group showed a more concentrated distribution near the median (Fig. 3A). Gene Set Enrichment Analysis (GSEA) revealed significant enrichment in PEDV-infected samples, with the most prominent pathways being “Cytokine-cytokine receptor interaction" and "JAK-STAT signaling pathway” (Fig. 3B-D). These findings suggest that PEDV infection significantly impacts genes related to cytokine-cytokine receptor interactions and the JAK-STAT signaling pathway. Furthermore, this implies that the host may exert its antiviral defense against PEDV by regulating innate immune pathways such as cytokine-cytokine receptor interactions and the JAK-STAT signaling pathway.

To further investigate the correlation between PEDV infection and the JAK-STAT signaling pathway, Circos plots and volcano plots were generated using the OmicStudio Cloud Platform (https://www.omicstudio.cn) and the Bioinformatics Platform (https://www.bioinformatics.com.cn), respectively. The Circos plot revealed significant correlations between PEDV infection and key components of the JAK-STAT pathway, including STAT1, MX1, ISG15, and OASL (Fig. 3E). Additionally, the volcano plot demonstrated that MX1, ISG15, and OASL were the most significantly upregulated genes following PEDV infection, followed by STAT1 (Fig. 3F). These findings suggest that the JAK-STAT signaling pathway in host cells plays a crucial role in mounting an immune defense during PEDV invasion.

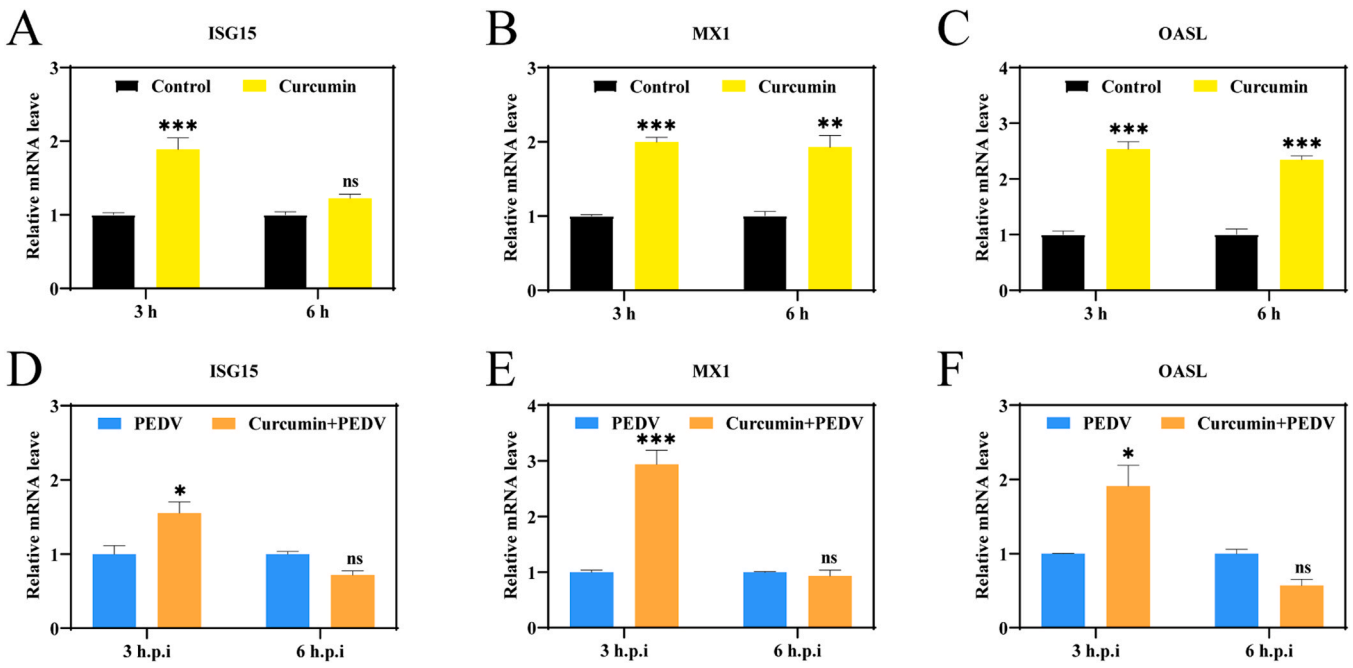

Fig. 7. Effects of Curcumin on the Transcription Levels of ISGs (ISG15, MX1, OASL) in IPEC-J2 Cells Under Normal Physiological Conditions and PEDV Infection. (A-C) Changes in the transcription levels of ISGs following curcumin treatment under normal physiological conditions. (D-F) Alterations in the transcription levels of ISGs in IPEC-J2 cells pretreated with curcumin prior to PEDV infection. Asterisks indicate significant differences (*: $P < 0.05$; **: $P < 0.01$; ***: $P < 0.001$; ns: not significant).

3.3. PEDV infection stimulates IPEC-J2 cells to secrete IFN-α, IFN-β

Type I IFN and Type III IFN exhibit differences in their induction kinetics. Specifically, IFN-α induces the expression of ISGs more rapidly, whereas IFN-λ exhibits a delayed but more sustained response (Ingle et al., 2018). Given that curcumin exerts its antiviral effects during the early stages of PEDV infection, we measured the expression levels of Type I IFN, namely IFN-α and IFN-β, following PEDV infection. Standard curves were plotted with the concentration of porcine IFN-α and IFN-β standards on the Y-axis and the OD450 values on the X-axis. The results showed a strong linear relationship between OD450 and the concentrations of IFN-α and IFN-β (Fig. S2-S3). ELISA results revealed that both IFN-α and IFN-β secretion levels increased in IPEC-J2 cells after PEDV infection. Notably, IFN-α levels peaked most significantly at 3 h.p.i., while IFN-β levels peaked most significantly at 6 h.p.i. (Fig. 4A-B).

3.4. PEDV infection activates the JAK-STAT signaling pathway and triggers the transcription of ISGs in IPEC-J2 Cells

As previously mentioned, although PEDV infection employs multiple mechanisms to evade IFN-mediated innate immune responses, the host cell's innate antiviral immune system can still actively respond to viral infection. Moreover, IFN-mediated innate immunity remains a critical defense mechanism against viral infections (Raftery and Stevenson, 2017). The results showed that following PEDV infection, the transcriptional levels of STAT1, its phosphorylation status, and its nuclear localization were significantly increased in IPEC-J2 cells. Specifically, the transcriptional level of STAT1 peaked most significantly at 3 h.p.i. (Fig. 5A), while the total STAT1 protein levels were significantly elevated at both 3 h.p.i. and 6 h.p.i., with phosphorylation levels peaking most notably at 6 h.p.i. (Fig. 5B-D). Additionally, nuclear localization of STAT1 was significantly increased at both 3 h.p.i. and 6 h.p.i. (Fig. 5E-J). RT-qPCR results further demonstrated that the transcriptional levels of ISG15 and OASL were significantly upregulated in IPEC-J2 cells after PEDV infection. Notably, ISG15 transcription peaked most significantly at 6 h.p.i., while MX1 transcription showed an upward trend at both 3 h.p.i. and 6 h.p.i., and OASL transcription was significantly elevated at 6 h.p.i. (Fig. 5K-M). These findings indicate that PEDV infection activates the IFN-α- and IFN-β-mediated JAK-STAT signaling cascade in the early stages of IPEC-J2 cell infection, as evidenced by the corresponding increase in downstream effector molecules.

3.5. Curcumin activates the JAK-STAT signaling pathway in IPEC-J2 cells to enhance innate immunity

It is well established that curcumin exhibits remarkable efficacy in modulating immune function (Tripathy et al., 2021). Under normal physiological conditions, treatment with curcumin significantly increased the levels of IFN-α and IFN-β in IPEC-J2 cells at both 3 h and 6 h post-treatment, with the most pronounced increase observed at 3 h (Fig. 4C-D). Further analysis using RT-qPCR, Western blot, and IFA revealed significant increases in the transcriptional levels of STAT1 (Fig. 6A), the phosphorylation levels of STAT1 protein (Fig. 6B-D), and the nuclear localization of STAT1 (Fig. 6E-J). Notably, the transcriptional levels of STAT1 peaked at 6 h, while both the phosphorylated protein levels and nuclear localization showed significant increases at both 3 h and 6 h. Furthermore, the transcriptional levels of ISG15, MX1, and OASL were also significantly upregulated (Fig. 7A-C). Collectively, these results demonstrate that curcumin enhances the innate immune response of host cells by promoting the secretion of IFN-α and IFN-β and activating the JAK-STAT signaling pathway in IPEC-J2 cells.

3.6. Curcumin activates the JAK-STAT signaling pathway in IPEC-J2 cells to inhibit PEDV replication

As previously mentioned, compared to the negative control group, the secretion levels of IFN-α and IFN-β were elevated in the PEDV-infected group. However, under PEDV infection conditions with curcumin pretreatment, the levels of IFN-α and IFN-β in the cells were further increased at both 3 h.p.i. and 6 h.p.i. compared to the PEDV-infected group (Fig. 4E-F). This indicates that curcumin significantly enhances

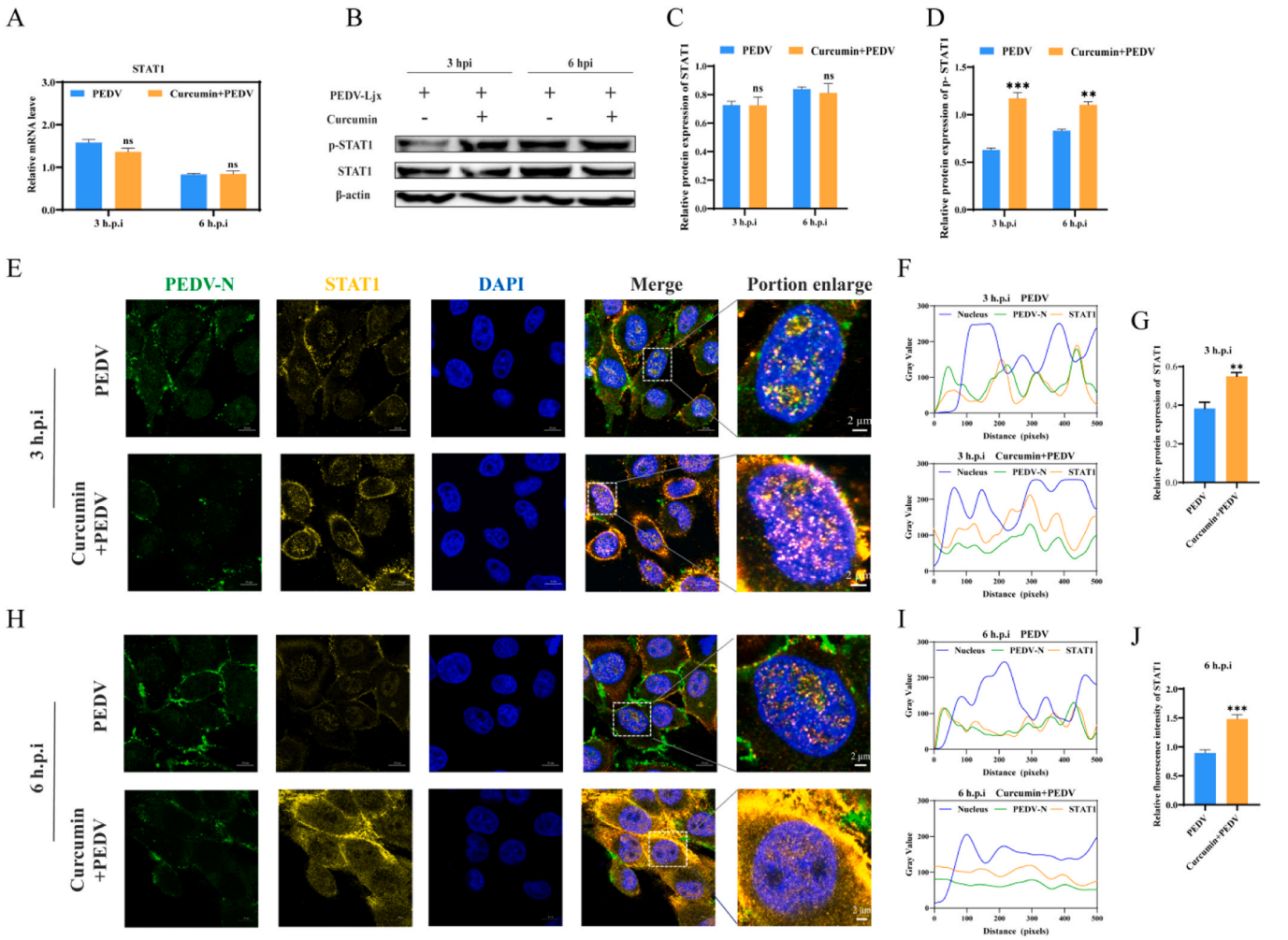

Fig. 8. Changes in STAT1 under Curcumin pretreatment of PEDV infection conditions. (A) Changes in 3 h.p.i., 6 h.p.i. STAT1 transcript levels. (B-D) Changes in 3 h.p.i., 6 h.p.i. STAT1 total protein level, phosphorylated protein level. (E-J) Changes in STAT1 localization in the nucleus of 3 h.p.i., 6 h.p.i. cells. Asterisks in the figure indicate significant differences (*: $P < 0.05$; **: $P < 0.01$; ***: $P < 0.001$; ns: not significant).

the expression of Type I IFN following PEDV infection. ISG15, MX1, and OASL are key antiviral proteins that exert their antiviral effects through distinct mechanisms. ISG15, an ubiquitin-like protein, is one of the most widely expressed ISGs induced by IFN-α. MX1 plays a crucial role in trapping viral nucleocapsids entering the cell, while OASL enhances innate antiviral immune responses (Raftery and Stevenson, 2017). Compared to the negative control group, the PEDV-infected group showed significant increases in ISG15 and OASL levels, with MX1 exhibiting an upward trend. Additionally, the transcriptional levels of STAT1, its phosphorylation status, and its nuclear localization were significantly elevated. In contrast, under PEDV infection conditions with curcumin pretreatment, the transcriptional levels of ISG15, MX1, and OASL were all increased at 3 h.p.i. (Fig. 7D-F). Although the transcriptional level of STAT1 in IPEC-J2 cells showed no significant change (Fig. 8A), its phosphorylation status (Fig. 8B-D) and nuclear localization (Fig. 8E-J) were significantly enhanced. These results demonstrate that curcumin further promotes STAT1 phosphorylation and nuclear translocation after PEDV infection. Collectively, these findings suggest that curcumin inhibits PEDV replication by enhancing the host cell's JAK-STAT signaling pathway.

3.7. Curcumin protects against PEDV infection and prevents diarrhea in piglets

To determine the antiviral effects of curcumin against PEDV in vivo and its impact on the JAK-STAT signaling pathway, we conducted a clinical trial using Rongchang piglets as an animal model to evaluate curcumin as a preventive agent against PEDV and to validate its mechanism of action (Fig. 9A). Clinical symptoms of the piglets were observed daily from 0 to 3 d post-viral infection. The results showed that piglets in the PEDV-infected group exhibited severe diarrhea, accompanied by clinical signs such as lethargy, loss of appetite, and rough hair. In contrast, preventive administration of curcumin resulted in well-formed feces, significantly alleviated diarrhea, and improved mental status compared to the PEDV-positive group. Neither the negative control group nor the curcumin-treated group showed obvious clinical symptoms. All piglets were euthanized 3 d post-infection. Postmortem examination revealed that the gastrointestinal tracts of piglets pretreated with curcumin showed no significant pathological changes compared to those of the PEDV-infected group (Fig. 9B). RT-qPCR analysis of viral load in the jejunum of each piglet demonstrated that the PEDV viral content in the curcumin-protected group was significantly lower than that in the PEDV-positive group (Fig. 9C). Western blot results further confirmed that the levels of PEDV N protein in the jejunum of the curcumin-protected group were significantly reduced compared to the PEDV-positive group (Fig. 9D-E). These results strongly indicate that preventive use of curcumin effectively alleviates diarrhea, improves mental status, and significantly mitigates intestinal damage caused by PEDV in piglets.

RT-qPCR was performed to measure the expression levels of genes

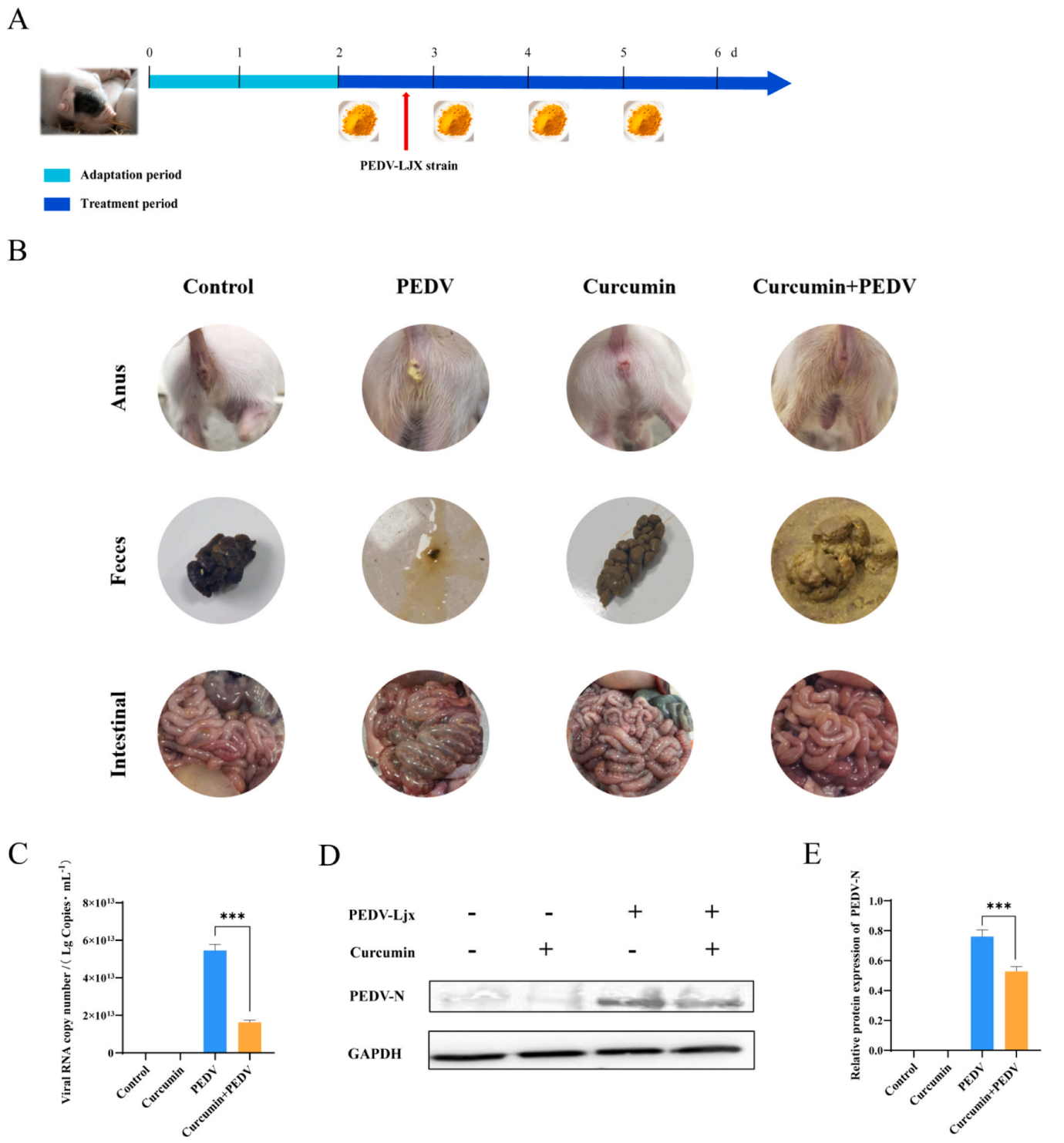

Fig. 9. Clinical protection effect of Curcumin on PEDV-infected piglets. (A) Schematic diagram of the animal experiment process. (B) The clinical effect of curcumin in preventing PEDV infection was evaluated from three aspects: the degree of buttocks contamination, fecal morphology and intestinal lesions in piglets. (C) Detection of viral content in intestinal tissues (jejunum) of piglets by RT-qPCR. (D) Western blot of PEDV N protein levels in piglet jejunal tissues. (E) Quantitative analysis of PEDV N protein levels in piglet jejunal tissues. Asterisks in the figure indicate significant differences (*: $P < 0.05$; **: $P < 0.01$; ***: $P < 0.001$; ns: not significant).

associated with the JAK-STAT pathway in the jejunal tissues of each piglet. The results showed that, compared to the negative control group, the transcriptional levels of STAT1, ISG15, MX1, and OASL were significantly elevated in the curcumin-treated group, PEDV-positive group, and curcumin-protected group. Notably, compared to the PEDV-positive group, the curcumin-protected group exhibited significantly higher transcriptional levels of STAT1, ISG15, MX1, and OASL (Fig. 10A, E-G). Western blot analysis revealed that the total STAT1 protein levels and phosphorylation status were significantly increased in the curcumin-treated group, PEDV-positive group, and curcumin-protected group compared to the negative control group. Moreover, the phosphorylation levels of STAT1 in the curcumin-

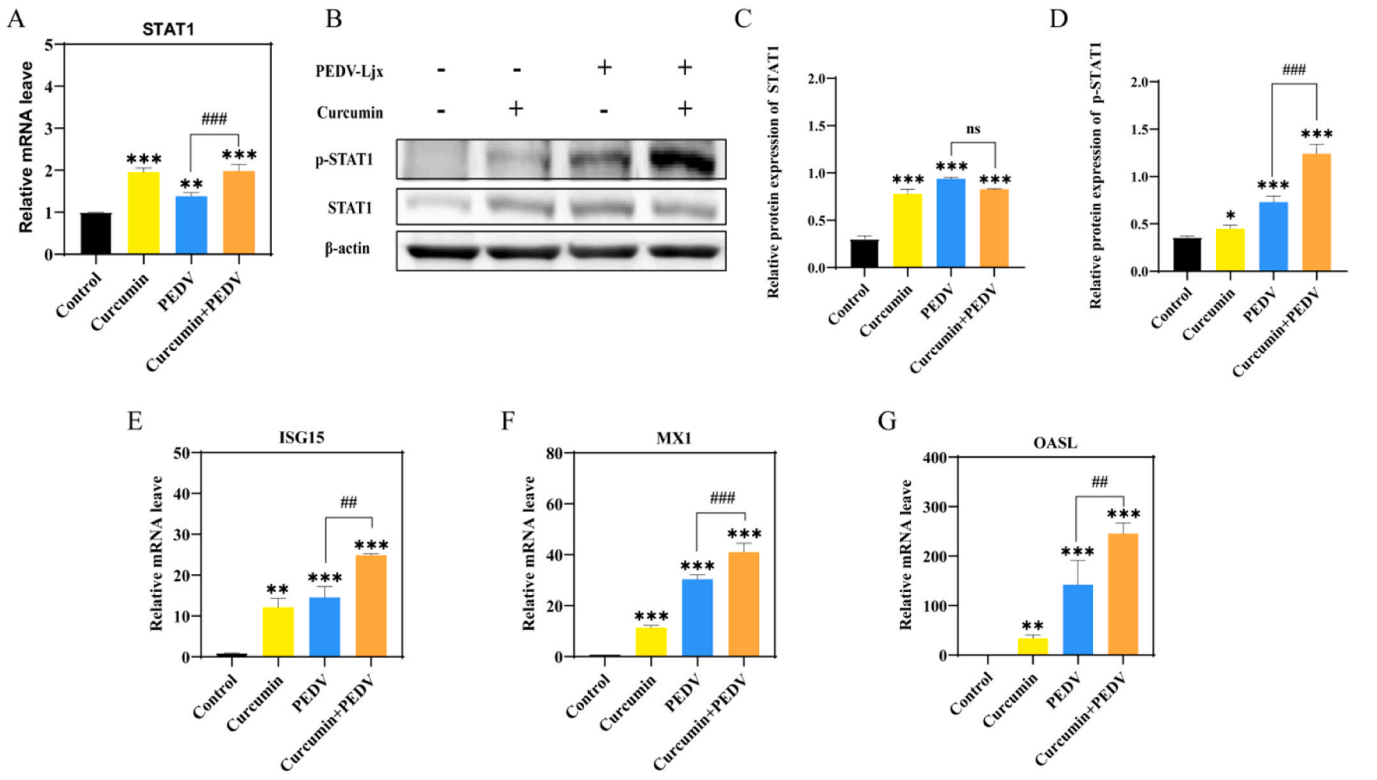

Fig. 10. Effects of Curcumin on JAK-STAT signaling pathway in piglets. (A) Transcript levels of STAT1 in piglet jejunal tissues. (B) Western blotting of STAT1 total protein level and phosphorylated protein level in piglet jejunal tissues. (C-D) Quantitative analysis of total and phosphorylated protein levels of STAT1 in piglet jejunal tissues. (E-G) Transcript levels of ISG15, MX1 and OASL in piglet jejunal tissues. Asterisks in the figure indicate significant differences (*: $P < 0.05$; **: $P < 0.01$; ***: $P < 0.001$; ns: not significant).

protected group were particularly elevated compared to the PEDV-positive group (Fig. 10B-D). These findings are consistent with the in vitro experimental results and further demonstrate that curcumin exhibits potent clinical antiviral efficacy in preventing and controlling PEDV. Additionally, these results reaffirm that curcumin activates the JAK-STAT signaling pathway in vivo to enhance innate immune responses, thereby exerting its anti-PEDV effects.

4. Discussion

PED is one of the most serious swine diseases, and its pathogen PEDV belongs to coronaviruses with high mutation characteristics. Since 2010, the mutated strains of PEDV have been widely spread in China, which has caused serious economic losses to the country's swine farming industry (Wang et al., 2016). With the continuous updating and prevalence of PEDV variants, the effectiveness of traditional vaccines continues to decrease, therefore, the development of anti-PEDV drugs has become a top priority for the prevention of PEDV infection. In this study, we found that curcumin showed favorable anti-PEDV activity both in vivo and in vitro.

The host's innate immune response serves as the first line of defense against viral invasion. Upon viral infection, the induction of IFN-α and IFN-β represents one of the most rapid and effective responses by the host to initiate innate immunity. These interferons activate the JAK-STAT signaling pathway by binding to specific receptors, leading to the induction of hundreds of ISGs and the establishment of an antiviral state (Philips et al., 2022), thereby defending against viral invasion. Through transcriptomic analysis, this study predicted a correlation between PEDV and the JAK-STAT signaling pathway, suggesting that the host activates the JAK-STAT-mediated innate immune response upon PEDV infection. To further validate this conclusion, we used IPEC-J2 cells as an in vitro model to investigate changes in IFN-α, IFN-β, STAT1, ISG15, MX1, and OASL following PEDV infection. The results showed that the secretion levels of IFN-α and IFN-β, upstream components of the JAK-STAT signaling pathway, were elevated after PEDV infection, with IFN-α being more sensitive to PEDV invasion. Additionally, the transcriptional levels, phosphorylation status, and nuclear localization of STAT1, a midstream component of the pathway, were increased. Furthermore, the transcriptional levels of downstream ISGs, including ISG15, MX1, and OASL, were also elevated. These findings indicate that IPEC-J2 cells, upon PEDV infection, produce IFN-α and IFN-β, which activate the JAK-STAT-mediated innate immune response to combat viral infection. The results of this study are consistent with those of Chen et al., who reported that PEDV infection induces the production of Type I/III IFN and upregulates the phosphorylation and non-phosphorylation levels of STAT1 protein, as well as the transcriptional levels of STAT1, MX1, and ISG15 in LLC-PK1 cells (Chen et al., 2022). Additionally, studies have shown that PEDV infection significantly increases the levels of p-STAT1 and p-STAT3 in IPEC-J2 cells (Yang et al., 2022), which aligns with the findings of Hu et al., who observed a significant increase in STAT1 transcriptional levels during PEDV infection (Hu et al., 2020). However, conflicting results have also been reported, such as the downregulation of STAT1 expression at 24 and 48 h post-PEDV infection (Guo et al., 2016), and the lack of significant changes in STAT1 during in vivo PEDV infection, as demonstrated by Li et al. (Li et al., 2016). These discrepancies may arise from differences in infection time points, cell lines, or experimental animal models used. Furthermore, this study revealed that PEDV infection induces earlier and more abundant secretion of IFN-α compared to IFN-β. Interestingly, this was accompanied by upregulation of STAT1 transcriptional levels, phosphorylation status, and nuclear localization, suggesting that IFN-α may play a more prominent role in regulating the JAK-STAT signaling pathway. However, this hypothesis requires further validation.

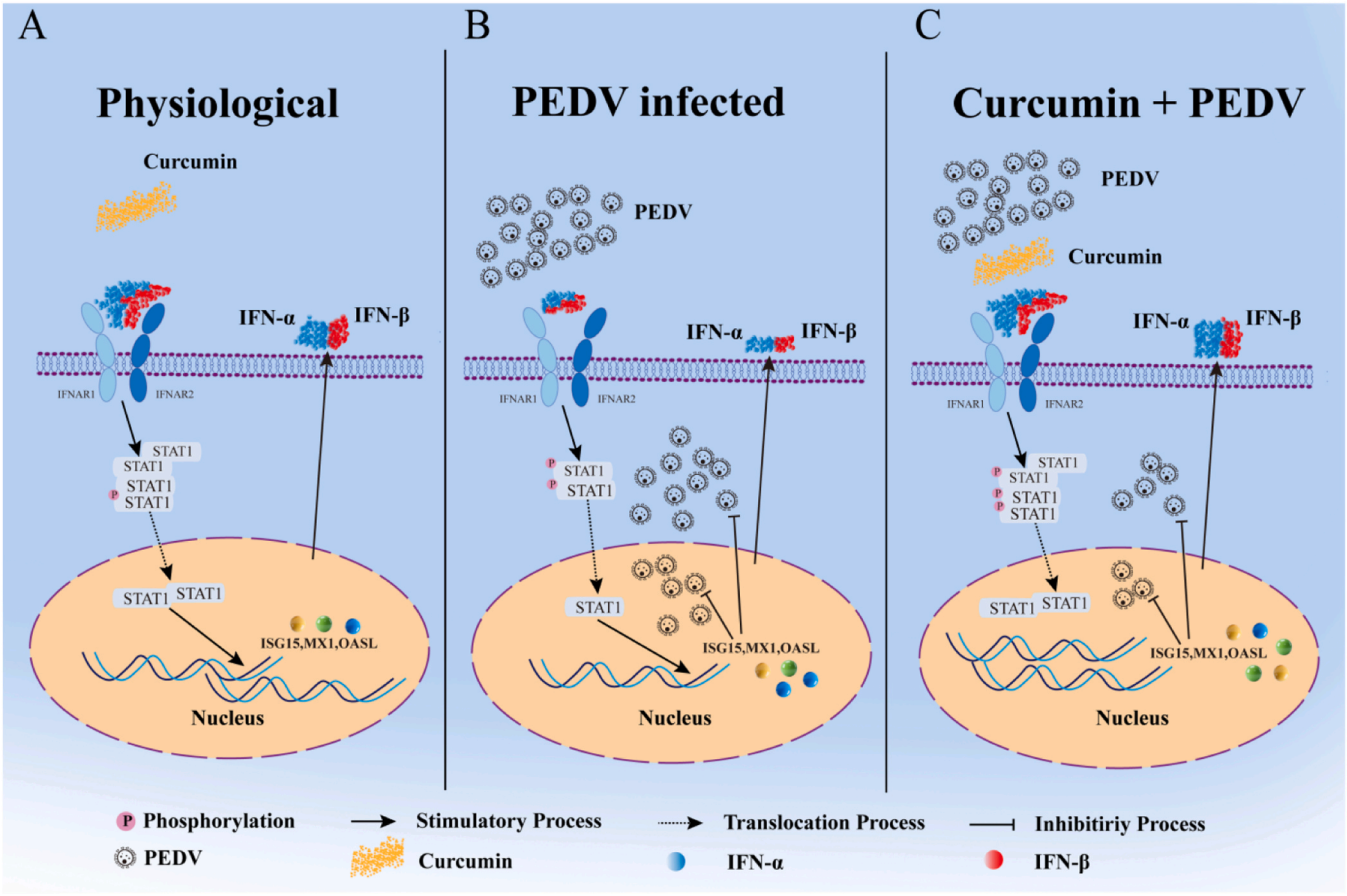

Fig. 11. Schematic diagram of curcumin's anti-PEDV infection mechanism via the JAK-STAT signaling pathway.

Curcumin, a natural pigment extracted from the rhizomes of plants belonging to the Zingiberaceae and Araceae families, has garnered significant attention across various industries due to its diverse biological functions, including anti-inflammatory, antimicrobial, antitumor, antioxidant, and antiviral properties. Recent studies have revealed that curcumin exhibits antiviral activity against a variety of viruses. Curcuminoids can inhibit the replication of dengue virus (DENV) by suppressing lipogenesis (Balasubramanian et al., 2019), and a curcumin-PSSNa conjugate has been shown to interact with Zika virus (ZIKV) particles, preventing viral attachment and thereby hindering the infection process (Obłoza et al., 2024). Curcumin has also been demonstrated to exert inhibitory effects at multiple stages of the SARS-CoV-2 lifecycle and exhibits virucidal properties (Marín-Palma et al., 2021). It is well-known that the SARS-CoV-2 spike (S) protein binds to the host cell receptor ACE2 to facilitate cellular entry (Lan et al., 2020). Based on computational molecular docking results, curcumin shows strong binding affinity to both the SARS-CoV-2 S protein and the host ACE2 protein, with binding energies of −7.9 kcal/mol and −7.8 kcal/mol, respectively. Multiple chemical interactions, including van der Waals forces, hydrogen bonds, and carbon-hydrogen bonds, have been identified between curcumin and the S protein as well as the ACE2 protein (Jena et al., 2021). Additionally, studies have demonstrated that curcumin exhibits antiviral and virucidal effects against TGEV, another member of the coronavirus family. Different treatment approaches indicate that curcumin not only inhibits the adsorption and replication stages of TGEV but also exerts virucidal effects in a dose-dependent manner (Li et al., 2020). These findings suggest that curcumin can manifest distinct antiviral mechanisms depending on the host cells and viruses involved. Although the in vitro and in vivo data have shown that curcumin has potent anti-PEDV effects, further experiments are necessary to elucidate the specific lifecycle stage of PEDV targeted by curcumin and to explore its detailed antiviral mechanisms in depth.

The type I IFN cascade is a robust immune defense mechanism of host cells and plays a critical role in combating viral infections (Ivashkiv and Donlin, 2014). Many viruses have evolved various strategies to interfere with or evade the host innate immune response (Cai et al., 2025; Wang et al., 2019). During viral infection, TBK1 and IRF3, as key effector molecules, are crucial for inducing IFN production. It has been reported that PEDV nsp15 can degrade the RNA of TBK1 and IRF3, thereby disrupting the host IFN response (Wu et al., 2020). FBXW7 is a positive innate antiviral factor that enhances the expression of RIG-I and TBK1 and promotes the production of ISGs. PEDV nsp2 can degrade FBXW7 protein in target cells via the ubiquitin-proteasome pathway, thereby suppressing the host antiviral response (Li et al., 2022). The PEDV N protein can inhibit IFN-β production by interfering with the interaction between IRF3 and TBK1 (Ding et al., 2014). Guo et al. found that the levels of p-STAT1 were elevated during the early stages of PEDV infection (1–24 h) but rapidly decreased after 24 h, with an even earlier decline observed in IPEC-J2 cells (Guo et al., 2016). Here, we confirmed that both the cellular p-STAT1 levels and the nuclear localization of STAT1 were significantly increased at 6 h.p.i. under PEDV infection conditions, which further demonstrates that PEDV activates the host IFN response during the early stages of infection. However, as the infection progresses, the IFN response gradually weakens. Compared to cells not infected with PEDV but treated with IFN-α, cells infected with PEDV for 36 h and then treated with IFN-α showed almost no p-STAT1 band (Guo et al., 2016). The inability to activate STAT1 with IFN-α during the late stages of PEDV infection suggests that PEDV interferes with the type I IFN-mediated JAK-STAT signaling pathway by inhibiting STAT1 phosphorylation. These results collectively demonstrate a close relationship between PEDV infection and the type I IFN-mediated JAK-STAT

signaling pathway. Therefore, modulating factors related to the JAK-STAT signaling pathway may represent a novel strategy to reduce PEDV immune evasion.

In summary, this study is the first to demonstrate that curcumin can effectively inhibit PEDV infection both in vivo and in vitro. Our research revealed that although PEDV infection activates the type I IFN-mediated JAK-STAT signaling pathway in host cells, the host's innate antiviral immune response is insufficient to counteract PEDV invasion due to the virus's potent immune evasion mechanisms. However, treatment with curcumin significantly suppressed PEDV infection. Curcumin was found to stimulate the secretion of IFN-α and IFN-β in IPEC-J2 cells prior to viral infection, promoting the activation of the JAK-STAT signaling pathway and enhancing the transcription of ISGs, thereby boosting the host's innate immune capacity to resist PEDV infection (Fig. 11). Surprisingly, under PEDV infection conditions, the promotive effect of curcumin pretreatment on ISG transcription gradually diminished over time. This phenomenon may be attributed to the low bioavailability of curcumin, which is rapidly metabolized by the body, thus preventing sustained stimulation of the JAK-STAT signaling pathway. Therefore, designing more effective delivery methods for curcumin and its analogs, such as utilizing nanotechnology for curcumin delivery (Butnariu et al., 2022), to enhance its bioavailability and maximize its immunostimulatory and antiviral effects will be a key focus of future research.

CRediT authorship contribution statement

Cao Lijing: Project administration, Investigation, Funding acquisition. **Liu Xiangyang:** Writing – original draft, Visualization, Validation, Software, Methodology, Formal analysis, Data curation. **Lei Chenghong:** Writing – review & editing, Supervision, Project administration, Investigation, Funding acquisition, Conceptualization. **Yuan Jianbo:** Writing – original draft, Visualization, Validation, Software, Data curation. **Song Zhenhui:** Writing – review & editing, Supervision, Project administration, Funding acquisition, Data curation, Conceptualization. **Wang Jing:** Validation, Software, Data curation. **Jiang Qiancheng:** Writing – review & editing, Writing – original draft, Visualization, Validation, Software, Methodology, Formal analysis. **Li Fei:** Visualization, Validation, Formal analysis. **Zhang Xingcui:** Writing – review & editing, Supervision, Project administration, Investigation, Data curation, Conceptualization. **Zhang Shujuan:** Visualization, Validation, Supervision, Formal analysis, Data curation. **Zhang Yiling:** Visualization, Software, Methodology, Formal analysis, Data curation. **Kan Zifei:** Validation, Software, Formal analysis, Data curation. **Hu Xia:** Visualization, Validation, Software, Data curation. **Zhou Yang:** Visualization, Software, Formal analysis. **Niu Zheng:** Validation, Supervision, Methodology, Formal analysis, Data curation. **Zhang Li:** Visualization, Validation, Software, Data curation.

Declaration of Competing Interest

The authors declare that the research was conducted in the absence of any commercial or financial relationships that could be construed as a potential conflict of interest.

Acknowledgements

This work was supported by the Venture & Innovation Support Program for Chongqing Overseas Returnees (cx2019097).

Appendix A. Supporting information

Supplementary data associated with this article can be found in the online version at doi:10.1016/j.vetmic.2025.110535.

References

Aaronson, D.S., Horvath, C.M., 2002. A road map for those who don't know JAK-STAT. Science 296, 1653–1655.
Balasubramanian, A., Pilankatta, R., Teramoto, T., Sajith, A.M., Nwulia, E., Kulkarni, A., Padmanabhan, R., 2019. Inhibition of dengue virus by curcuminoids. Antivir. Res 162, 71–78.
Butnariu, M., Quispe, C., Koirala, N., Khadka, S., Salgado-Castillo, C.M., Akram, M., Anum, R., Yeskaliyeva, B., Cruz-Martins, N., Martorell, M., Kumar, M., Vasile Bagiu, R., Abdull Razis, A.F., Sunusi, U., Muhammad Kamal, R., Sharifi-Rad, J., 2022. Bioactive effects of curcumin in human immunodeficiency virus infection along with the most effective isolation techniques and type of nanoformulations. Int J. Nanomed. 17, 3619–3632.
Cai, Z., Ni, W., Li, W., Wu, Z., Yao, X., Zheng, Y., Zhao, Y., Yuan, W., Liang, S., Wang, Q., Tang, M., Chen, Y., Lan, K., Zhou, L., Xu, K., 2025. SARS-CoV-2 S protein disrupts the formation of ISGF3 complex through conserved S2 subunit to antagonize type I interferon response. J. Virol. 99, e0151624.
Chen, P., Zhu, J., Yu, J., Liu, R., Lao, M., Yu, L., Gao, F., Jiang, Y., Liu, C., Tong, W., Liu, H., Tong, G., Zhou, Y., 2022. Porcine epidemic diarrhea virus strain FJzz1 infection induces type I/III IFNs production through RLRs and TLRs-mediated signaling. Front Immunol. 13, 984448.
Decker, T., Müller, M., Stockinger, S., 2005. The yin and yang of type I interferon activity in bacterial infection. Nat. Rev. Immunol. 5, 675–687.
Ding, Z., Fang, L., Jing, H., Zeng, S., Wang, D., Liu, L., Zhang, H., Luo, R., Chen, H., Xiao, S., 2014. Porcine epidemic diarrhea virus nucleocapsid protein antagonizes beta interferon production by sequestering the interaction between IRF3 and TBK1. J. Virol. 88, 8936–8945.
Gao, Y., Hu, J.H., Liang, X.D., Chen, J., Liu, C.C., Liu, Y.Y., Cheng, Y., Go, Y.Y., Zhou, B., 2021. Curcumin inhibits classical swine fever virus replication by interfering with lipid metabolism. Vet. Microbiol 259, 109152.
Guo, L., Luo, X., Li, R., Xu, Y., Zhang, J., Ge, J., Bu, Z., Feng, L., Wang, Y., 2016. Porcine epidemic diarrhea virus infection inhibits interferon signaling by targeted degradation of STAT1. J. Virol. 90, 8281–8292.
Hu, Z., Li, Y., Du, H., Ren, J., Zheng, X., Wei, K., Liu, J., 2020. Transcriptome analysis reveals modulation of the STAT family in PEDV-infected IPEC-J2 cells. BMC Genom. 21, 891.
Ingle, H., Peterson, S.T., Baldridge, M.T., 2018. Distinct effects of type I and IIi interferons on enteric viruses. Viruses 10.
Ivashkiv, L.B., Donlin, L.T., 2014. Regulation of type I interferon responses. Nat. Rev. Immunol. 14, 36–49.
Jena, A.B., Kanungo, N., Nayak, V., Chainy, G.B.N., Dandapat, J., 2021. Author correction: catechin and curcumin interact with S protein of SARS-CoV2 and ACE2 of human cell membrane: insights from computational studies. Sci. Rep. 11, 8482.
Lan, J., Ge, J., Yu, J., Shan, S., Zhou, H., Fan, S., Zhang, Q., Shi, X., Wang, Q., Zhang, L., Wang, X., 2020. Structure of the SARS-CoV-2 spike receptor-binding domain bound to the ACE2 receptor. Nature 581, 215–220.
Liang, J., Xu, W., Pan, X., Han, S., Zhang, L., Wen, H., Ding, M., Zhang, W., Peng, D., 2024. Advances research in porcine enteric coronavirus therapies and antiviral drugs. Vet. Q 44, 1–49.
Li, Z., Chen, F., Ye, S., Guo, X., Muhanmmad Memon, A., Wu, M., He, Q., 2016. Comparative proteome analysis of porcine jejunum tissues in response to a virulent strain of porcine epidemic diarrhea virus and its attenuated strain. Viruses 8.
Li, W., Li, H., Liu, Y., Pan, Y., Deng, F., Song, Y., Tang, X., He, Q., 2012. New variants of porcine epidemic diarrhea virus, China, 2011. Emerg. Infect. Dis. 18, 1350–1353.
Li, Y., Wang, J., Liu, Y., Luo, X., Lei, W., Xie, L., 2020. Antiviral and virucidal effects of curcumin on transmissible gastroenteritis virus in vitro. J. Gen. Virol. 101, 1079–1084.
Li, M., Wu, Y., Chen, J., Shi, H., Ji, Z., Zhang, X., Shi, D., Liu, J., Tian, J., Wang, X., Shi, Z., Zhang, H., Zhang, H., Guo, L., Feng, L., 2022. Innate immune evasion of porcine epidemic diarrhea virus through degradation of the FBXW7 protein via the ubiquitin-proteasome pathway. J. Virol. 96, e0088921.
Mahjoor, M., Mahmoudvand, G., Farokhi, S., Shadab, A., Kashfi, M., Afkhami, H., 2023. Double-edged sword of JAK/STAT signaling pathway in viral infections: novel insights into virotherapy. Cell Commun. Signal 21, 272.
Marín-Palma, D., Tabares-Guevara, J.H., Zapata-Cardona, M.I., Flórez-Álvarez, L., Yepes, L.M., Rugeles, M.T., Zapata-Builes, W., Hernandez, J.C., Taborda, N.A., 2021. Curcumin inhibits in vitro SARS-CoV-2 infection In Vero E6 cells through multiple antiviral mechanisms. Molecules 26.
Nittayananta, W., Lerdsamran, H., Chutiwitoonchai, N., Promsong, A., Srichana, T., Netsomboon, K., Prasertsopon, J., Kerdto, J., 2024. A novel film spray containing curcumin inhibits SARS-CoV-2 and influenza virus infection and enhances mucosal immunity. Virol. J. 21, 26.
Obłoza, M., Milewska, A., Botwina, P., Szczepański, A., Medaj, A., Bonarek, P., Szczubiałka, K., Pyrć, K., Nowakowska, M., 2024. Curcumin-poly(sodium 4-styrenesulfonate) conjugates as potent zika virus entry inhibitors. ACS Appl. Mater. Interfaces 16, 5426–5437.
Philips, R.L., Wang, Y., Cheon, H., Kanno, Y., Gadina, M., Sartorelli, V., Horvath, C.M., Darnell Jr., J.E., Stark, G.R., O'Shea, J.J., 2022. The JAK-STAT pathway at 30: Much learned, much more to do. Cell 185, 3857–3876.
Raftery, N., Stevenson, N.J., 2017. Advances in anti-viral immune defence: revealing the importance of the IFN JAK/STAT pathway. Cell Mol. Life Sci. 74, 2525–2535.
Schneider, W.M., Chevillotte, M.D., Rice, C.M., 2014. Interferon-stimulated genes: a complex web of host defenses. Annu Rev. Immunol. 32, 513–545.
Tripathy, S., Verma, D.K., Thakur, M., Patel, A.R., Srivastav, P.P., Singh, S., Gupta, A.K., Chávez-González, M.L., Aguilar, C.N., Chakravorty, N., Verma, H.K., Utama, G.L., 2021. Curcumin extraction, isolation, quantification and its application in functional

foods: a review with a focus on immune enhancement activities and COVID-19. Front Nutr. 8, 747956.
Wang, D., Chen, J., Yu, C., Zhu, X., Xu, S., Fang, L., Xiao, S., 2019. Porcine reproductive and respiratory syndrome virus nsp11 antagonizes type I interferon signaling by targeting IRF9. J. Virol. 93.
Wang, D., Fang, L., Xiao, S., 2016. Porcine epidemic diarrhea in China. Virus Res 226, 7–13.
Wang, Z., Li, X., Shang, Y., Wu, J., Dong, Z., Cao, X., Liu, Y., Lan, X., 2020. Rapid differentiation of PEDV wild-type strains and classical attenuated vaccine strains by fluorescent probe-based reverse transcription recombinase polymerase amplification assay. BMC Vet. Res 16, 208.
Wang, X., Wang, X., Zhang, J., Shan, Q., Zhu, Y., Xu, C., Wang, J., 2023. Prediction and verification of curcumin as a potential drug for inhibition of PDCoV replication in LLC-PK1 cells. Int J. Mol. Sci. 24.
Wood, E.N., 1977. An apparently new syndrome of porcine epidemic diarrhoea. Vet. Rec. 100, 243–244.
Wu, Y., Zhang, H., Shi, Z., Chen, J., Li, M., Shi, H., Shi, D., Guo, L., Feng, L., 2020. Porcine epidemic diarrhea virus nsp15 antagonizes interferon signaling by RNA degradation of TBK1 and IRF3. Viruses 12.
Xu, J., Gao, Q., Zhang, W., Zheng, J., Chen, R., Han, X., Mao, J., Shan, Y., Shi, F., He, F., Fang, W., Li, X., 2023. Porcine epidemic diarrhea virus antagonizes host IFN-λ-mediated responses by tilting transcription factor STAT1 toward acetylation over phosphorylation to block its activation. mBio 14, e0340822.
Yang, J., Chen, D., Tian, G., Mao, X., He, J., Zheng, P., Yu, J., Luo, Y., Luo, J., Huang, Z., Wu, A., Yan, H., Yu, B., 2022. 1,25-dihydroxyvitamin D(3) negatively regulates the inflammatory response to porcine epidemic diarrhea virus infection by inhibiting NF-κB and JAK/STAT signaling pathway in IPEC-J2 porcine epithelial cells. Int J. Mol. Sci. 23.
Zhang, J., Yuan, S., Peng, Q., Ding, Z., Hao, W., Peng, G., Xiao, S., Fang, L., 2022. Porcine epidemic diarrhea virus nsp7 inhibits interferon-induced JAK-STAT signaling through sequestering the interaction between KPNA1 and STAT1. J. Virol. 96, e0040022.